

NOTES

Construction and Characterization of a Human T-Cell Lymphotropic Virus Type 3 Infectious Molecular Clone[▽]

Sébastien Alain Chevalier,^{1,4} Nga Ling Ko,¹ Sara Calattini,¹ Adeline Mallet,² Marie-Christine Prévost,² Kylene Kehn,³ John N. Brady,⁴ Fatah Kashanchi,³ Antoine Gessain,¹ and Renaud Mahieux^{1,3*}

Unité d'Epidémiologie et Physiopathologie des Virus Oncogènes, CNRS URA 3015, Département de Virologie, Institut Pasteur, 28 rue du Dr. Roux, 75015 Paris, France¹; Plateforme de Microscopie Electronique, Institut Pasteur, 25 rue du Dr. Roux, 75015 Paris, France²; Department of Microbiology, Immunology and Tropical Medicine and Department of Biochemistry, The George Washington University Medical Center, Washington, DC 20037³; and NIH/NCI/LCO/VTB, Bethesda, Maryland 20892⁴

Received 4 February 2008/Accepted 8 April 2008

We and others have uncovered the existence of human T-cell lymphotropic virus type 3 (HTLV-3). We have now generated an HTLV-3 proviral clone. We established that *gag*, *env*, *pol*, *pro*, and *tax/rex* as well as minus-strand mRNAs are present in cells transfected with the HTLV-3 clone. HTLV-3 p24^{gag} protein is detected in the cell culture supernatant. Transfection of 293T-long terminal repeat (LTR)-green fluorescent protein (GFP) cells with the HTLV-3 clone promotes formation of syncytia, a hallmark of Env expression, together with the appearance of fluorescent cells, demonstrating that Tax is expressed. Viral particles are visible by electron microscopy. These particles are infectious, as demonstrated by infection experiments with purified virions.

Phylogenetic analyses have provided supporting evidence that multiple episodes of interspecies virus transmission have occurred between nonhuman primates and humans (9, 16). Examples are human T-lymphotropic viruses (HTLVs) and their related simian counterparts (STLVs) that all belong to the primate T-cell lymphotropic viruses (8, 10, 23). STLV type 3 (STLV-3) was isolated in 1994 from a captive baboon (*Papio hamadryas*) (7). It is now well established that STLV-3 strains are widespread in a number of simian species living in West, East, and Central Africa (5, 7, 12–15, 18–22). HTLV type 3 (HTLV-3), the human counterpart of STLV-3, was discovered in 2005 by our laboratory and another (3, 17, 24), and a third strain has been described more recently (1). We sequenced the 8,553-bp genome of an HTLV-3 strain (HTLV-3_{Py143}) (2) and showed that it is very similar to that of STLV-3_{CTO604}, a simian strain from Cameroon (14). However, sequence comparisons also revealed that the HTLV-3_{Py143} genome is shorter than the STLV-3 sequences, due to a 366-bp deletion in the pX proximal region. Of note, this deletion does not affect *tax*, *rex*, or *env* sequences (2).

Using a PCR-based strategy, we recently developed the first infectious STLV-3 molecular clone (4). Here, we have employed the same strategy to construct an HTLV-3 molecular clone, with HTLV-3_{Py143} DNA as a source of proviral material. In a first series of experiments, we generated the full-length 8,853-bp HTLV-3_{Py143} provirus by PCR amplification of 20 overlapping fragments as previously described (4). The provi-

ral sequence was ligated into the SV2_{neo} plasmid between the EcoRI and HpaI restriction sites (Fig. 1A, top panel). Clones were then screened by digesting the plasmids with EcoRI plus BamHI plus ScaI or with PstI or XbaI (Fig. 1A, top, middle, and bottom panels). Two clones (SV2_{Py143 c19} and SV2_{Py143 c126}) displayed the expected restriction digestion pattern (Fig. 1B, lanes 2 to 3, 5 to 6, and 8 and 9), indicating that these plasmids contained the full-length HTLV-3_{Py143} provirus. Full sequence analysis was also performed on both clones and demonstrated that neither mutations nor deletions that would alter the different viral protein sequences had been introduced in the HTLV-3_{Py143} provirus during the cloning process (data not shown).

We then determined whether our molecular clone was capable of directing mRNA synthesis in cell culture. To this end, SV2_{Py143 c19} and SV2_{Py143 c126} plasmids were transfected into 293T cells as described previously (4). After 2 days, total RNA was extracted and treated twice with DNase I. Reverse transcription-PCR experiments were then performed to detect different mRNA viral species—*gag*, *pro*, and *pol* (nonspliced); *env* (singly spliced); and *tax/rex* (doubly spliced)—as well as a putative mRNA transcribed from the minus strand of the genome. This mRNA could be translated into a protein that we tentatively named AEP (antisense-encoded protein).

Total RNA (0.5 μg) was used as a matrix for reverse transcriptase PCR (RT-PCR) with the OneStep RT-PCR kit (Qiagen). PCR was performed using the following primer pairs: for *Gag*, LTR681s (GGAGAAAGCAAACAGGTGGGGG) and GAG1119as (GTGGGGGTGAAGGACAGGGAGG) (459-bp RT-PCR product); for *Pro*, Pro2016se (5'-AGGACTAACCTCCCCCGGACC-3') and Pro2412as (5'-GAGAACTTGA GGGTTGGTCAGC-3') (397-bp RT-PCR product); for *Pol*, Pol4029s (5'-CCATCCACCCAGTGTGACCTACAC-3') and Pol4633as (5'-GGTTGTAGGGAACATGGGTTGAAT-3')

* Corresponding author. Mailing address: INSERM, Unité d'Epidémiologie et Physiopathologie des Virus Oncogènes, CNRS URA 3015, Institut Pasteur, 28 rue du Docteur Roux, 75724 Paris cedex 15, France. Phone: (33) 1-45-68-89-06. Fax: (33) 1-40-61-34-65. E-mail: rmahieux@pasteur.fr.

[▽] Published ahead of print on 16 April 2008.

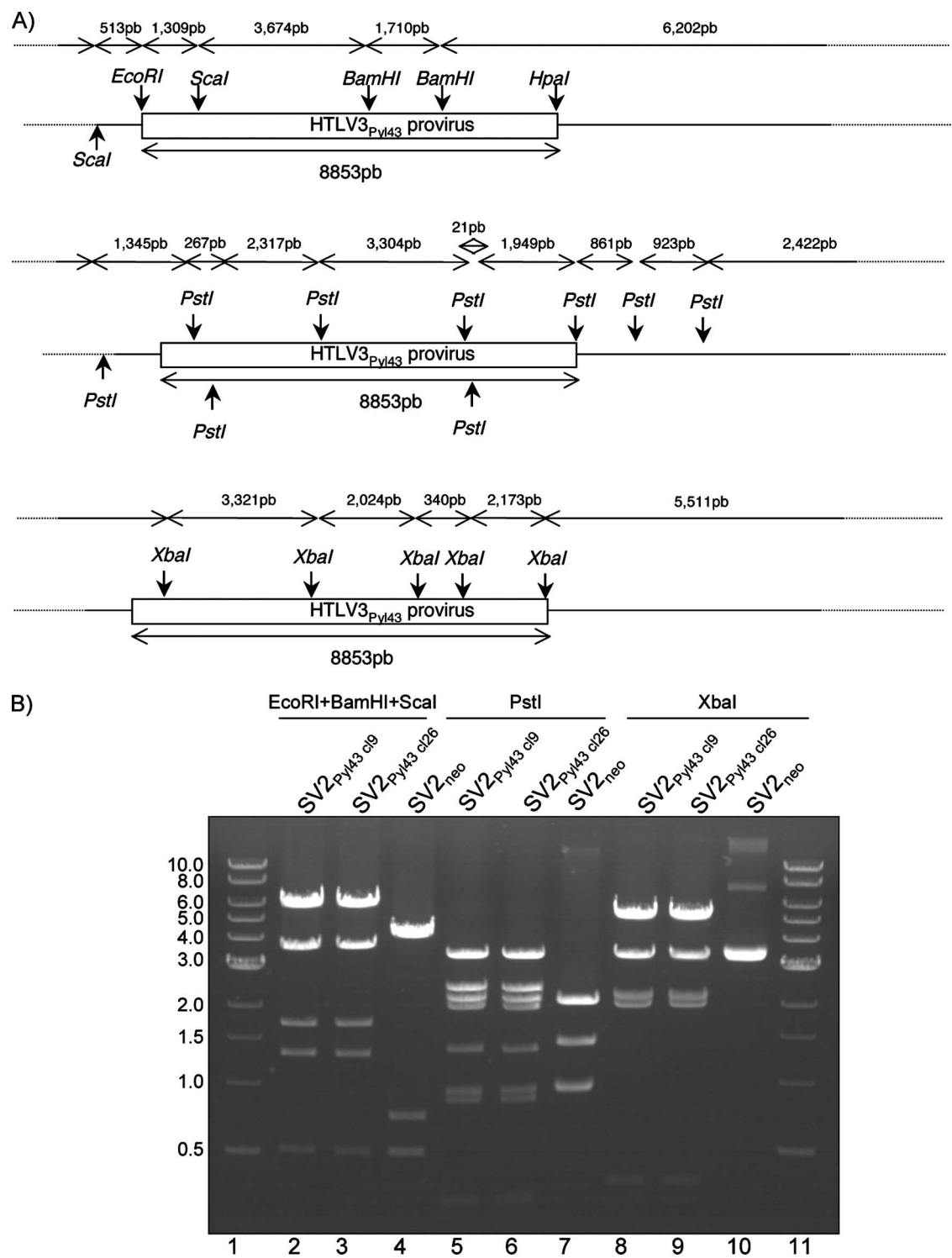


FIG. 1. Construction of the SV2_{Pyl43} clone and expression of the viral mRNAs in vivo. (A) Restriction map of the full-length HTLV-3_{Pyl43} genome inserted into the SV2_{neo} plasmid. (B) Lanes 1 and 11, 1-kb DNA ladder; lanes 2, 3, and 4, restriction profiles of SV2_{Pyl43} cl9, SV2_{Pyl43} cl26, and SV2_{neo} backbone plasmids digested with EcoRI plus ScaI plus BamHI and run on a 0.7% agarose gel; lanes 5, 6, and 7, plasmids digested with PstI; lanes 8, 9, and 10, plasmids digested with XbaI. pb, paired bases.

(605-bp RT-PCR product); for Env, LTR111s (CCAAGGCTC TGACGTCTCTCCCTAC) and Env5117as (TGGGATTGCC AAAAGAGGAAGGG) (516-bp RT-PCR product); for Tax, 602LTR and 602MVB Rex (14) (424-bp RT-PCR product);

and for AEP, Pyl43-AEPs (5'-GGAGGCTCCAACCTCAGG-3') and Pyl43-AEPas (5'-ACTCCGCCACTTCCTGTAG-3') (274-bp RT-PCR product).

As seen in Fig. 2A (lanes 4 and 5, top, middle, and bottom

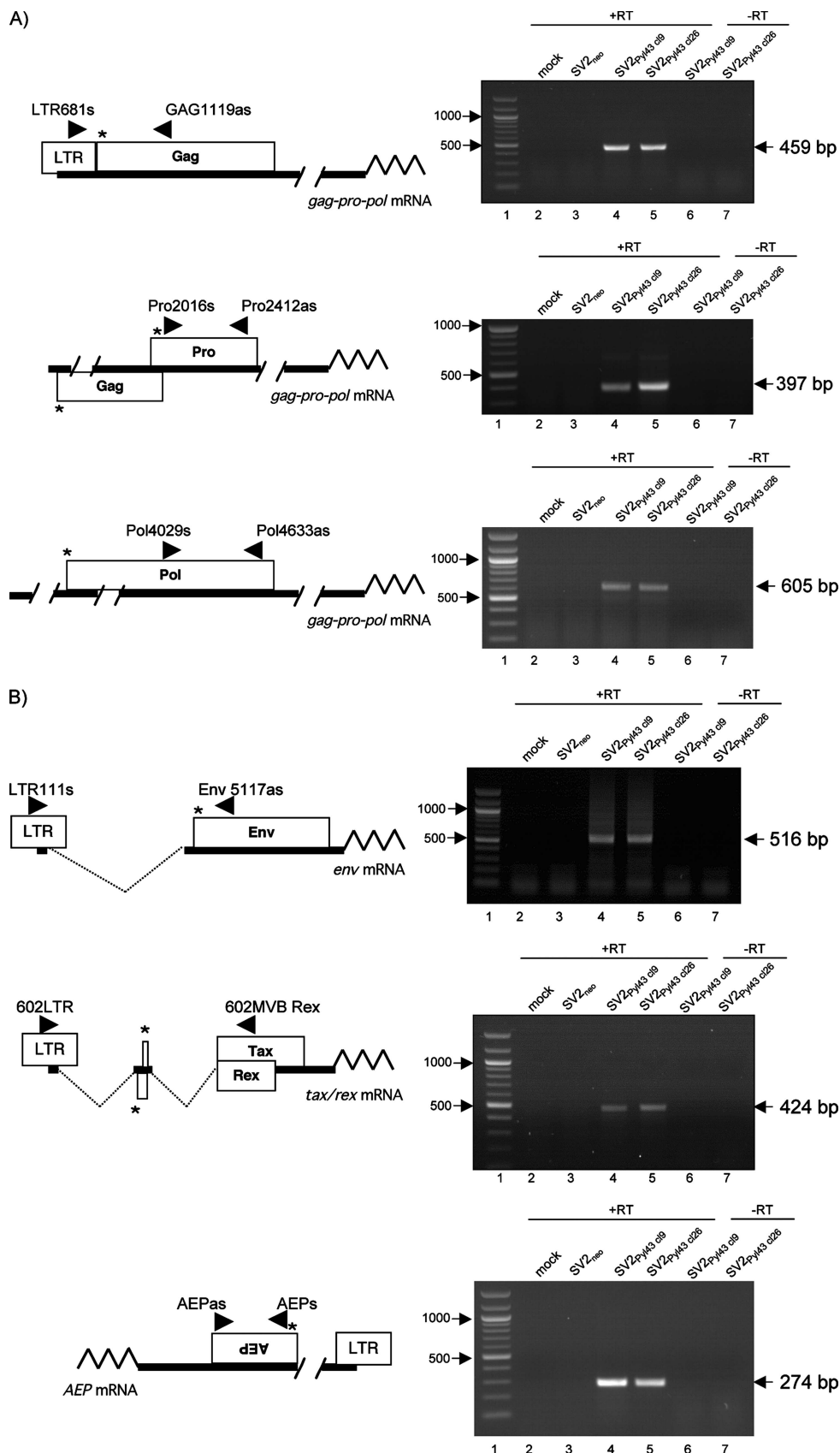
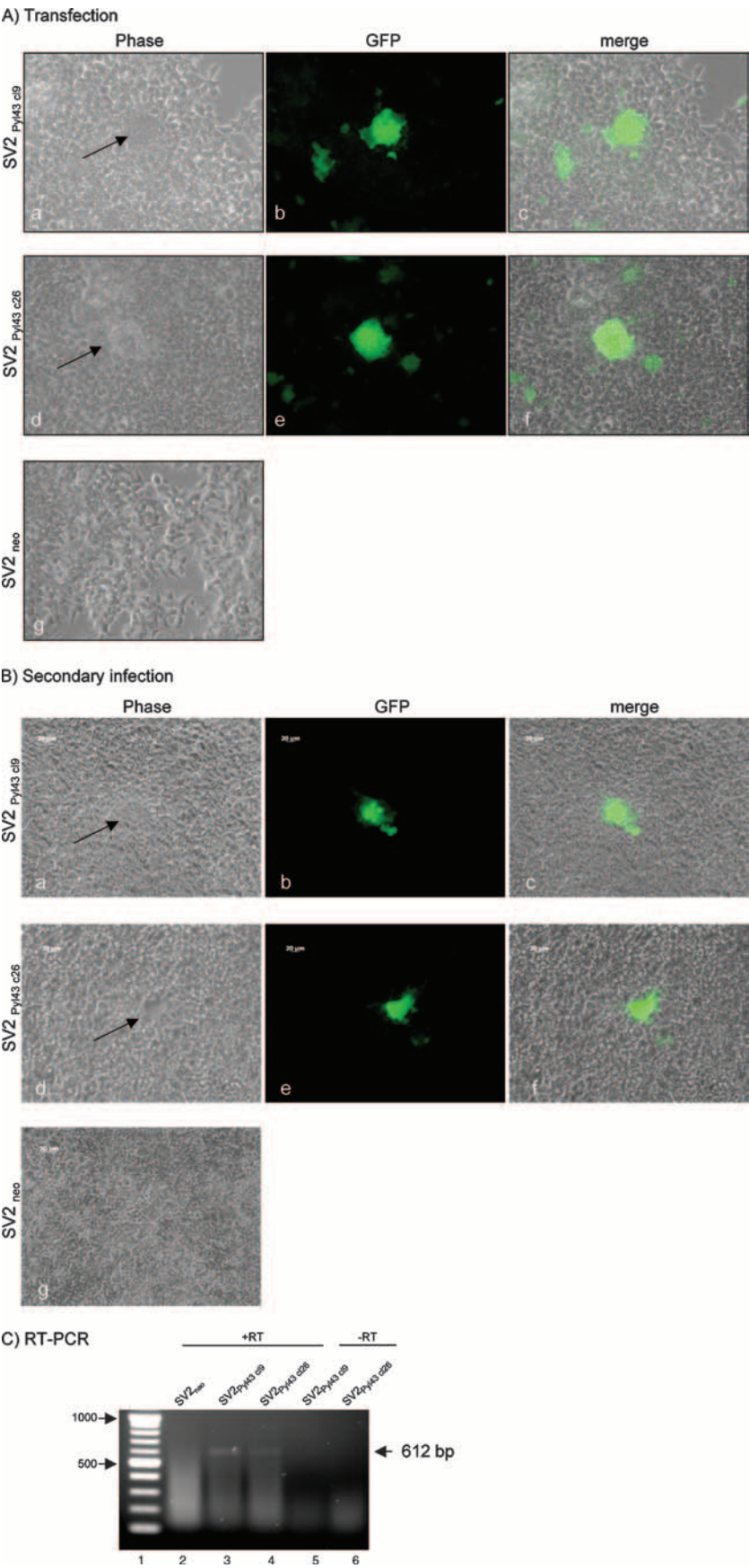


FIG. 2. HTLV-3_{Py143} provirus is transcribed in vitro. (A and B) RT-PCR analysis of SV2_{Py143} viral RNAs. Total RNA was extracted from 293T cells transfected with SV2_{Py143 c19}, SV2_{Py143 c26}, and SV2_{neo} plasmids or mock transfected. (A) Top, *gag*; middle, *pro*; and bottom, *pol*. (B) Top, *env*; middle, *tax/rex*; bottom, *AEP*. (A and B) Lanes 1, 100-bp DNA ladder; lane 2, mock-transfected 293T cells; lane 3, RNA from SV2_{neo} (backbone vector)-transfected cells; lanes 4 to 7, RNA from cells transfected with SV2_{Py143 c19} and SV2_{Py143 c26} plasmids in the presence (lanes 4 and 5) or absence (lanes 6 and 7) of RT. *, ATG.



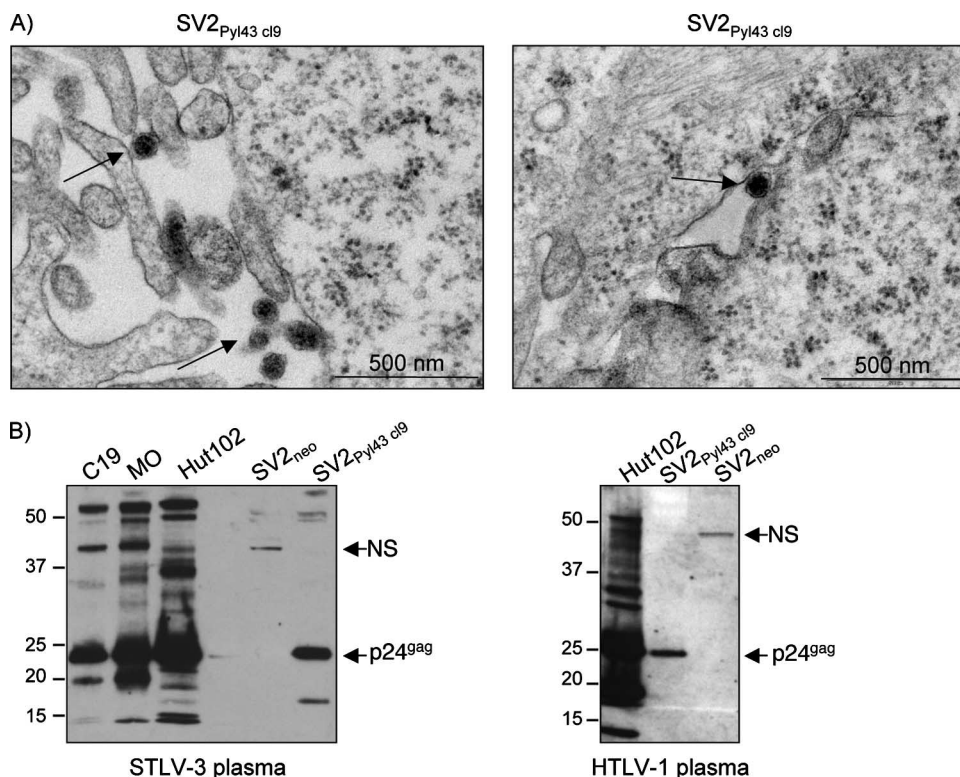


FIG. 4. (A) Electron micrograph showing HTLV-3_{Py143} particles in SV2_{Py143} cl9-transfected cells. (B) Expression of HTLV-3 p24^{gag} protein. 293T cells were transfected with SV2_{Py143} cl9 or SV2_{neo} plasmid. Growth medium was collected. After lysis, viral proteins were transferred to a membrane and incubated with plasma obtained from an STLV-3-infected monkey (PPA-F8) (left) or plasma obtained from an HTLV-1-infected TSP/HAM patient (PH1378) (right). These Western blots are representative of three different experiments.

panels), an HTLV-3-specific band corresponding to different part of the *gag pro pol* transcript was present only in extracts obtained from SV2_{Py143}-transfected cells. The absence of a PCR product when RT was omitted demonstrates the lack of DNA carryover in the RNA preparation (Fig. 2A, lanes 6 and 7, top, middle, and bottom panels). *env* and *tax/rex* transcripts were also present in these cell extracts (Fig. 2B, top and middle panels). Finally, we also demonstrated that, as in HTLV-1, the HTLV-3 minus strand is transcribed (Fig. 2B, bottom panel). Whether the protein that is translated from this mRNA is functionally related to HBZ remains to be determined. Next, 293T-long terminal repeat (LTR)-green fluorescent protein (GFP) indicator cells (6) were transfected with either the SV2_{Py143} cl9 or SV2_{Py143} cl26 plasmid.

The appearance of syncytia is linked to the interaction of the viral envelope on the surface of the infected cells with the viral receptors that are present on the surface of adjacent cells. Forty-eight hours posttransfection, cell culture medium was removed. Cells were washed with phosphate-buffered saline

and fixed, and pictures were taken with a Zeiss Axioplan-Axiocam-apotome system (Fig. 3A). As expected, syncytium formation was observed after transfection of SV2_{Py143} cl9 or SV2_{Py143} cl26 plasmid in the 293T-LTR-GFP cells demonstrating HTLV-3 envelope expression (Fig. 3A, panels a and d). These syncytia were GFP positive (Fig. 3A, panels b and c and e and f), therefore establishing that the Tax protein was expressed and able to transactivate the viral promoter in these cells. GFP signal and syncytia were not visible in cells transfected with the empty backbone vector (Fig. 3A, panel g).

To determine whether SV2_{Py143}-transfected cells produce infectious particles, cell culture supernatant was collected from SV2_{Py143} cl9- or SV2_{Py143} cl26-transfected cells, purified, and added to 293T-LTR-GFP indicator cells as previously described (4) (Fig. 3B). After several days of culture, a number of GFP-positive syncytia were reproducibly observed (Fig. 3B, panels a and d). These syncytia were GFP positive (panels b and c and e and f). As a control, we did not observe any syncytia when 293T-LTR-GFP cells were put in contact with

FIG. 3. Viral envelope and Tax expression. (A) 293T-LTR-GFP indicator cells were transiently transfected with SV2_{Py143} cl9 (a to c), SV2_{Py143} cl26 (d to f), or SV2_{neo} (g) backbone vector. The images shown are representative of three different experiments. (B) SV2_{Py143} viral particles are infectious. Growth medium was collected from cells transfected with SV2_{Py143} cl9 (a to c), SV2_{Py143} cl26 (d to f), or SV2_{neo} (g) molecular clones and added to 293T-LTR-GFP indicator cells as previously described (4). The images are representative of three different experiments. (C) RT-PCR analysis of SV2_{Py143} viral RNA extracted from cells infected with purified HTLV-3 viral particles. Lane 1, 100-bp DNA ladder; lane 2, RNA from SV2_{neo} (backbone vector)-transfected cells; lanes 3 to 6, RNA from cells transfected with SV2_{Py143} cl9 and SV2_{Py143} cl26 plasmids in the presence (lanes 3 and 4) or absence (lanes 5 and 6) of RT.

supernatant from cells transfected with the backbone vector (Fig. 3B, panel g). We also performed RT-PCR on the RNA extracted from cells infected with cell-free virus. RNA was extracted and reverse transcribed as described above. PCR was then performed with primers located within the *gag* open reading frame: LTR681s (5'-GGAGAAAGCAAACAGGTGGGGG G-3') and Gag1293as (5'-TCATGGAGATCTTTAGCTGTG GGG-3' (PCR product of 612 bp).

This allowed us to demonstrate that *gag pro pol* mRNA was present in these cells (Fig. 3C). Altogether, these results demonstrate that the purified HTLV-3_{Py143} particles are infectious.

We also wanted to observe viral particles. Forty-eight hours posttransfection of 293T with the molecular clone, cell culture medium was removed and the cells were washed with phosphate-buffered saline and fixed for ultrastructural analyses as previously described (4). Viral particles were then detected in SV2_{Py143 c19}-transfected cells by electron microscopy (Fig. 4A) but not in the cells transfected with the backbone vector (data not shown). The size of these particles is roughly similar to that of STLV-3 particles (4).

Finally, the supernatant of 293T cells transfected with SV2_{Py143 c19} was analyzed (Fig. 4B). Growth medium was collected, clarified by low-speed centrifugation, and filtrated. Virus was then layered on a 20% glycerol gradient and centrifuged. The pellet was resuspended in lysis buffer. Each sample was resolved by electrophoresis on a 10% *N,N*-methylenebisacrylamide-Tris gel. As controls, the supernatant from HTLV-1-infected (Hut102) and/or HTLV-2-infected (C19, MO) cell cultures was also tested. The membrane was incubated using STLV-3 plasma (Fig. 4B, left panel) or HTLV-1 plasma (right panel). With both sera, a band corresponding to the HTLV-3 p24^{gag} protein was observed in the supernatant obtained from SV2_{Py143 c19}-transfected cells, but not in the protein extracts from SV2_{neo}-transfected cells. Interestingly, the STLV-3 plasma also allowed the detection of the HTLV-1 and HTLV-2 p24^{gag} protein (Fig. 4B, left panel).

Altogether, our data demonstrate that the SV2_{Py143 c19} molecular clone is functional and produces infectious viral particles. Comparison of the viral life cycles of both STLV-3 and HTLV-3 in a rabbit model (11) will now allow us to ascertain whether the 366-bp deletion impacts either viral infectivity or replication in vivo. Finally, given the fact that an HTLV-3-infected cell line is not yet available, this clone will be a unique and powerful tool that will allow us to investigate HTLV-3 protein expression and viral pathogenesis in vivo.

This work was supported by fellowships from le Ministère de la Recherche and from La Fondation pour la Recherche Médicale to S.A.C., from la Ligue Contre le Cancer to S.C., and from the Croucher Foundation to N.L.K. R.M. is supported by INSERM. This work was supported by grants from the Virus Cancer Prevention Association, from the Programme Interdisciplinaire CNRS Maladies Infectieuses Émergentes to R.M., and from an NIH grant (AI072495-01) to R.M. and F.K.

We thank B. Barbeau for help in designing the AEP primers.

REFERENCES

- Calattini, S., E. Betsem, A. Froment, S. Bassot, S. A. Chevalier, R. Mahieux, and A. Gessain. 2007. Identification and complete sequence analysis of a new HTLV-3 strain from South Cameroon. *AIDS Res. Hum. Retrovir.* 23:596.
- Calattini, S., S. A. Chevalier, R. Duprez, P. Afonso, A. Froment, A. Gessain, and R. Mahieux. 2006. Human T-cell lymphotropic virus type 3: complete nucleotide sequence and characterization of the human Tax3 protein. *J. Virol.* 80:9876–9888.
- Calattini, S., S. A. Chevalier, R. Duprez, S. Bassot, A. Froment, R. Mahieux, and A. Gessain. 2005. Discovery of a new human T-cell lymphotropic virus (HTLV-3) in Central Africa. *Retrovirology* 2:30.
- Chevalier, S. A., M. Walic, S. Calattini, A. Mallet, M.-C. Prevost, A. Gessain, and R. Mahieux. 2007. Construction and characterization of a full-length infectious simian T-cell lymphotropic virus type 3 molecular clone. *J. Virol.* 81:6276–6285.
- Courgnaud, V., S. Van Dooren, F. Liegeois, X. Pourrut, B. Abela, S. Loul, E. Mpoudi-Ngole, A. Vandamme, E. Delaporte, and M. Peeters. 2004. Simian T-cell leukemia virus (STLV) infection in wild primate populations in Cameroon: evidence for dual STLV type 1 and type 3 infection in agile mangabeys (*Cercocebus agilis*). *J. Virol.* 78:4700–4709.
- Delebecque, F., K. Pramberger, M.-C. Prevost, M. Brahic, and F. Tangy. 2002. A chimeric human T-cell lymphotropic virus type 1 with the envelope glycoprotein of Moloney murine leukemia virus is infectious for murine cells. *J. Virol.* 76:7883–7889.
- Goubau, P., M. Van Brussel, A. M. Vandamme, H. F. Liu, and J. Desmyter. 1994. A primate T-lymphotropic virus, PTLV-L, different from human T-lymphotropic viruses types I and II, in a wild-caught baboon (*Papio hamadryas*). *Proc. Natl. Acad. Sci. USA* 91:2848–2852.
- Guo, H. G., F. Wong-Stall, and R. C. Gallo. 1984. Novel viral sequences related to human T-cell leukemia virus in T cells of a seropositive baboon. *Science* 223:1195–1197.
- Hahn, B. H., G. M. Shaw, K. M. De Cock, and P. M. Sharp. 2000. AIDS as a zoonosis: scientific and public health implications. *Science* 287:607–614.
- Hunsmann, G., J. Schneider, H. Bayer, E. Jurkiewicz, and N. Yamamoto. 1984. Structural and epidemiological features of primate lymphotropic retroviruses. *Princess Takamatsu Symp.* 15:109–118.
- Lairmore, M. D., L. Silverman, and L. Ratner. 2005. Animal models for human T-lymphotropic virus type 1 (HTLV-1) infection and transformation. *Oncogene* 24:6005–6015.
- Liegeois, F., B. Lafay, W. M. Switzer, S. Locatelli, E. Mpoudi-Ngole, S. Loul, W. Heneine, E. Delaporte, and M. Peeters. 2008. Identification and molecular characterization of new STLV-1 and STLV-3 strains in wild-caught nonhuman primates in Cameroon. *Virology* 371:405–417.
- Meertens, L., and A. Gessain. 2003. Divergent simian T-cell lymphotropic virus type 3 (STLV-3) in wild-caught *Papio hamadryas papio* from Senegal: widespread distribution of STLV-3 in Africa. *J. Virol.* 77:782–789.
- Meertens, L., R. Mahieux, P. Maucière, J. Lewis, and A. Gessain. 2002. Complete sequence of a novel highly divergent simian T-cell lymphotropic virus from wild-caught red-capped mangabeys (*Cercocebus torquatus*) from Cameroon: a new primate T-lymphotropic virus type 3 subtype. *J. Virol.* 76:259–268.
- Meertens, L., V. Shanmugam, A. Gessain, B. E. Beer, Z. Tooze, W. Heneine, and W. M. Switzer. 2003. A novel, divergent simian T-cell lymphotropic virus type 3 in a wild-caught red-capped mangabey (*Cercocebus torquatus torquatus*) from Nigeria. *J. Gen. Virol.* 84:2723–2727.
- Slattery, J. P., G. Franchini, and A. Gessain. 1999. Genomic evolution, patterns of global dissemination, and interspecies transmission of human and simian T-cell leukemia/lymphotropic viruses. *Genome Res.* 9:525–540.
- Switzer, W. M., S. H. Qari, N. D. Wolfe, D. S. Burke, T. M. Folks, and W. Heneine. 2006. Ancient origin and molecular features of the novel human T-lymphotropic virus type 3 revealed by complete genome analysis. *J. Virol.* 80:7427–7438.
- Takemura, T., M. Yamashita, M. K. Shimada, S. Ohkura, T. Shotake, M. Ikeda, T. Miura, and M. Hayami. 2002. High prevalence of simian T-lymphotropic virus type L in wild Ethiopian baboons. *J. Virol.* 76:1642–1648.
- Van Brussel, M., P. Goubau, R. Rousseau, J. Desmyter, and A.-M. Vandamme. 1997. Complete nucleotide sequence of the new simian T-lymphotropic virus, STLV-PH969 from a Hamadryas baboon, and unusual features of its long terminal repeat. *J. Virol.* 71:5464–5472.
- Van Brussel, M., P. Goubau, R. Rousseau, J. Desmyter, and A. M. Vandamme. 1996. The genomic structure of a new simian T-lymphotropic virus, STLV-PH969, differs from that of human T-lymphotropic virus types I and II. *J. Gen. Virol.* 77:347–358.
- Van Dooren, S., M. Salemi, X. Pourrut, M. Peeters, E. Delaporte, M. Van Ranst, and A.-M. Vandamme. 2001. Evidence for a second simian T-cell lymphotropic virus type 3 in *Cercopithecus nictians* from Cameroon. *J. Virol.* 75:11939–11941.
- Van Dooren, S., V. Shanmugam, V. Bhullar, B. Parekh, A. M. Vandamme, W. Heneine, and W. M. Switzer. 2004. Identification in gelada baboons (*Theropithecus gelada*) of a distinct simian T-cell lymphotropic virus type 3 with a broad range of Western blot reactivity. *J. Gen. Virol.* 85:507–519.
- Verdonck, K., E. Gonzalez, S. Van Dooren, A. M. Vandamme, G. Vanham, and E. Gotuzzo. 2007. Human T-lymphotropic virus 1: recent knowledge about an ancient infection. *Lancet Infect. Dis.* 7:266–281.
- Wolfe, N. D., W. Heneine, J. K. Carr, A. D. Garcia, V. Shanmugam, U. Tamoufe, J. N. Torimiro, A. T. Prosser, M. Lebreton, E. Mpoudi-Ngole, F. E. McCutchan, D. L. Birt, T. M. Folks, D. S. Burke, and W. M. Switzer. 2005. Emergence of unique primate T-lymphotropic viruses among central African bushmeat hunters. *Proc. Natl. Acad. Sci. USA* 102:7994–7999.